IVYSPRING INTERNATIONAL PUBLISHER

Theranostics

2025; 15(5): 1864-1878. doi: 10.7150/thno.99490

Review

LAT1-specific PET radiotracers: Development and clinical experiences of a new class of cancer-specific radiopharmaceuticals

Arifudin Achmad[1,2,3]✉, Hirofumi Hanaoka[4,5], Holis Abdul Holik[2,6], Keigo Endo[7], Yoshito Tsushima[8], Achmad Hussein S. Kartamihardja[1,2]

1. Department of Nuclear Medicine and Molecular Theranostics, Faculty of Medicine, Universitas Padjadjaran, Bandung 40161, West Java, Indonesia.
2. Theranostic Radiopharmaceutical Research Collaboration Center, Universitas Padjadjaran, Sumedang 45363, West Java, Indonesia.
3. Oncology and Stem Cell Study Center, Faculty of Medicine, Universitas Padjadjaran, Bandung 40161, West Java, Indonesia.
4. Faculty of Medicine, Kansai Medical University, Hirakata 573-1010, Japan.
5. Department of Radiotheranostics, Gunma University Graduate School of Medicine, Maebashi 3718511, Japan.
6. Department of Pharmaceutical Analysis and Medicinal Chemistry, Faculty of Pharmacy, Universitas Padjadjaran, Sumedang 45363, West Java, Indonesia.
7. Kyoto College of Medical Science, Kyoto 6220041, Japan.
8. Department of Diagnostic Radiology and Nuclear Medicine, Gunma University Graduate School of Medicine, Maebashi 3178511, Gunma, Japan.

✉ Corresponding author: Arifudin Achmad, MD, PhD; **Postal address**: Jl. Pasir Kaliki (H.O.S Tjokroaminoto) 192, Bandung 40161, West Java, Indonesia; **E-mail**: a.achmad@unpad.ac.id.

Received: 2024.06.11; Accepted: 2024.11.05; Published: 2025.01.02

Abstract

The quest for a cancer-specific positron emission tomography (PET) tracer has been ongoing for decades. Current evidence shows that targeting amino acid metabolism dysregulation is a valid alternative cancer detection method and can complement the conventional approach, which relies on targeting increased glucose metabolism. The rate of amino acid metabolism in all major organs is mostly equally low and does not change in any physiological dynamics. The amino acid metabolism rate only spikes in malignant tissues. PET imaging targeting LAT1 (L-type amino acid transporter 1) demonstrated accurate cancer imaging of various cancer types with nearly negligible background uptake. LAT1 is a *pan-cancer* biomarker of amino acid metabolism dysregulation. The upregulated LAT1 expression in cancer cells depicts their dynamic behavior and aggressiveness. This review discussed PET radiotracers developed as a LAT1-specific agent and how this new class of cancer-specific radiopharmaceuticals could deliver PET images with clinical properties we yearn for, such as high specificity toward various malignancies, robust non-cancer exclusion (mainly inflammatory reactions), accurate malignant lesion delineation, representative therapeutic monitoring, and long-term prognostication.

Keywords: LAT1; PET; radiopharmaceutical; cancer; amino acid metabolism

Introduction

Positron emission tomography (PET) has existed for about a half-century, yet a true oncologic PET radiotracer with *pan-cancer* efficacy remains elusive. The 2-deoxy-2-[^{18}F]fluoro-D-glucose ([^{18}F]FDG) has been the dominant PET radiotracer for oncology since PET invention due to its high sensitivity for malignancies with enhanced glycolysis [1]. By 2015, [^{18}F]FDG PET is indicated in the evidence-based guidelines for six cancer types (lung, colorectal, lymphoma, head and neck, melanoma, and esophageal cancer) [2] and only recently for pediatric oncology (mainly lymphomas and sarcomas) and ovarian cancer [3, 4]. However, the cancer-specificity of [^{18}F]FDG is often compromised in slow-growing tumors, lesions adjacent to inflammations, or lesions located within organs with high-rate glycolysis, such as the brain and liver [1]. Thus, in nuclear neurooncology, [^{18}F]FDG is less useful than radiolabeled amino acids, which are more suitable for wider clinical scenarios [5, 6].

Since the early days of [^{18}F]FDG, hundreds of PET radiotracers that targeted oncologic molecular biomarkers such as metabolic dysregulation (amino acid, fatty acids, or lactate), cellular proliferation (synthesis of proteins, DNA, and cell membranes) or expression of various receptors, enzymes, and tumor-associated or tumor-specific antigens have been investigated [7]. However, only a handful have obtained regulatory approval for oncology and are routinely used worldwide: [^{68}Ga]Ga-DOTATATE, [^{68}Ga]Ga-PSMA, [^{18}F]NaF, [^{18}F]FDOPA, and [^{18}F]FLT [8]. Recently, we witnessed a breakthrough as fibroblast activation protein (FAP) inhibitor (FAPI)-based PET radiotracers being used to target cancer-associated fibroblasts in the stroma of desmoplastic solid tumors. In most cases, FAPI delivers a high-contrast image [9]. However, FAP is also expressed in chronic inflammations, benign tumors, and fibrosis [10]. FAPI is also less superior than [^{18}F]FDG in lymphoma and multiple myeloma [11, 12]. Despite their unique properties, none of these PET radiotracers have had the versatility to compete with [^{18}F]FDG as a general oncologic PET radiotracer [8].

L-type amino acid transporter 1 (LAT1) has been regarded as a *pan-cancer*, cancer-specific molecular target [13]. The drug discovery for LAT1 has been going on for years and has narrowed to a few compounds. We reviewed the development, application, and future potential of PET radiopharmaceuticals that have been proven or claimed as LAT1-specific PET radiotracers.

Choosing targets and tracer design for *pan-cancer*, cancer-specific PET radiotracer

Molecular target selection is paramount in designing *pan-cancer* PET radiotracers. The target should be overexpressed in various cancers and have negligible physiologic expression. The target should also be readily accessible for tracer uptake, thus often a cell surface protein. It has to be robust from enzymatic degradation, has a low turnover rate, and is not shed from the cells nor trapped within the cells [14]. On the other side, the PET radiotracer should have high specificity and affinity for the target, along with low/negligible nonspecific binding toward normal tissues and non-cancer pathologies. It should also be sufficiently hydrophilic for rapid and large-volume distribution throughout the body and fast plasma clearance [14]. Small molecules fit this purpose, and their structure often allows for ^{18}F radiolabeling suitable for routine PET use [15].

The upregulated amino acid transporters in cancer have long been attractive targets [16]. Four transporters stand out as potential *pan-cancer* targets: LAT1 (L-type amino acid transporter 1), ASCT2 (Alanine, Serine, Cysteine Transporter 2), SNAT1, and SNAT2 (Sodium-coupled Neutral Amino Acid Transporter 1 and 2) [13]. Their overexpression in multiple cancer types is summarized in **Table S1** (ranked according to the global cancer burden data from GLOBOCAN 2022) [17]). LAT1 (encoded by the SLC7A5 gene) is a transmembrane protein, a member of the system-L amino acid transporter family (LAT1-4). In some cancers, LAT1 expression increases along with the increase of ASCT2 expression. However, ASCT2 is physiologically expressed in normal tissues of the lungs, muscles, large intestine [18], and inflammatory T cells [19], making ASCT2 less ideal as a cancer molecular target. In contrast, the LAT1 protein expression level on the plasma membrane of normal tissue is significantly lower than in cancer cells [20, 21]. In some cancers, e.g., ovarian epithelial carcinoma, the LAT1 mRNA expression level may be up to 10–29 times higher than the normal cells, resulting in significantly higher LAT1 protein expression [22]. LAT1 protein overexpression is consistent across diverse cancers, including breast, lung, stomach, colorectal, liver, esophagus, pancreas, kidney, brain, ovarian cancer [23], and non-Hodgkin's lymphoma [24]. LAT1 expression is also intertwined with various cancer hallmarks, and, more importantly, no evidence to date that LAT1 expression is involved in tumor-promoting inflammation in the cancer microenvironment [25]. Therapeutic studies in various cancer cells and xenografts showed that LAT1-specific inhibition halts cancer proliferation [26].

Challenges in designing LAT1-targeting PET radiotracer

The main requirements for LAT1-targeting radiotracers are high affinity and selectivity to LAT1. They should not inhibit other amino acid transporters expressed in non-cancer cells or other pathologies. In fact, unlike glucose or fatty acid transport systems, the amino acid transport system is way more complex. Each amino acid transport system has heterogeneous substrate and transport mechanisms. On top of that, most amino acids are transported by more than one transporter [13, 20]. Thus, it is not surprising that almost all amino acid-based PET radiotracers lack selectivity toward a particular transport system, let alone a specific amino acid transporter (**Table 1**). The diagnostic performance in various clinical scenarios is detailed elsewhere [27].

Table 1. Amino acid PET radiotracers (reviewed in meta-analyses) and their respective transporters

Amino acid PET tracers	Amino acid transporter(s) responsible for uptake	Organs of high physiological uptake*	Cancer types
[^{11}C]MET	LAT1-4, SNAT1, SNAT2, SNAT4, ASCT2 [29, 30]	Liver, pancreas (↓), salivary glands, lachrymal glands, bone marrow, bowels, kidney, and bladder [31]	Brain [32] (glioma [33], high-grade glioma [34]), parathyroid adenoma [35], multiple myeloma [36]
[^{18}F]FET	LAT2 (dominant), $ATB^{0,+}$, System B^0, LAT1 (poor) [30]	Pancreas, kidneys, liver, heart, colon, and muscle [31]	Brain (high-grade glioma [34], recurrent glioma [37], metastases [38])
[^{18}F]FDOPA	LAT1 and LAT2 (similar affinity) [39]	Urinary bladder, gallbladder, biliary tract, pancreas, kidney, basal ganglia, liver, and adrenal glands [40]	Neuroendocrine tumors (multiple sites [41], intestinal neuroendocrine tumors [42], medullary thyroid cancer [43]), glioma [44]
[^{18}F]FACBC	ASCT2, SNAT2, LAT1, LAT2 [45]	Liver, pancreas (↓), heart, kidneys, spleen, allbladder, bone marrow (↓), adrenal glands, muscle (↑), and stomach [46]	Prostate (primary lesion and primary lymph node metastasis) [47], recurrent prostate cancer [48], high-grade glioma [49]
[^{18}F]FAMT	LAT1 [29]	Kidney and urinary bladder [50]	Various cancer [51]

Notes: * Ranked from the highest, (↓)/(↑) decreased/increased uptake over time.

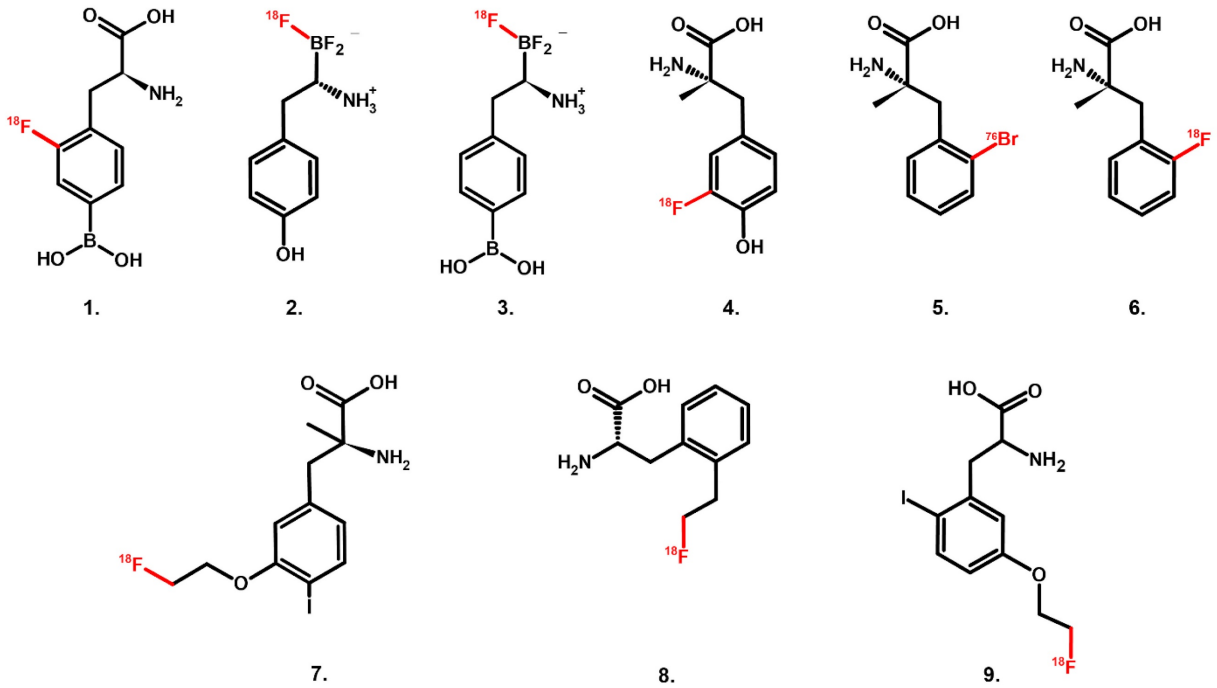

Figure 1. Chemical structure of PET radiotracers with high selectivity towards LAT1; **1.** [^{18}F]FBPA, **2.** [^{18}F]FBY, **3.** [^{18}F]BBPA, **4.** [^{18}F]FAMT, **5.** [^{76}Br]BAMP, **6.** [^{18}F]FAMP, **7.** [^{18}F]FIMP, and **8.** [^{18}F]FELP, and **9.** [^{18}F]NKO-035.

The amino acid transport mechanism is often *bi-directional* (*influx* of one amino acid is mandatory coupled with *efflux* of another amino acid) [28]. Thus, using radiolabeled amino acids plainly as PET radiotracers is challenging just by relying on their substrate characteristics. Bi-directional transport leads to a high washout rate; consequently, tumor uptake and retention may not be adequate, compromising its sensitivity. On the other hand, compounds that have a long history of LAT1-selective substrate or inhibitors (e.g., melphalan, gabapentin, T3 hormone) do not always have a strong LAT1 affinity [20].

The requirement for LAT1 recognition and the spectrum from substrate-type toward inhibitor-type of LAT1-selective compounds have been roughly mapped. A LAT1 substrate should possess at least an intact amino group, a carbonyl oxygen and alkoxy oxygen of the carboxyl group, and a hydrophobic side chain. Adding an α-methyl group into aromatic amino acids renders a compound a LAT1-selective substrate at the price of decreasing its LAT1 affinity. On the other end of the spectrum, high-affinity LAT1 inhibitors should have an α-amino acid structure with free carboxyl and amino groups and a hydrophobic bulky side chain, where the carbonyl oxygen of the carboxyl group should not be involved in intramolecular hydrogen bonding. Adding O-linked hydrophobic bulky moiety at the *para*-position of the aromatic ring is suggested as crucial to retaining LAT1-selectivity while having high affinity. However, hydrophobic moieties can sometimes remove the LAT1-selectivity entirely [20]. The LAT1-specific PET radiotracers discussed here mostly belong to the substrate-type compound (**Figure 1**). Phenylalanine

has long been known as a LAT1 high-affinity substrate (K_m = 14.2 μM) [52]. In order to develop an ideal LAT1-specific PET radiotracer based on LAT1 substrates, plasma amino acid concentrations should also be considered [53] (See **Graphical Abstract**). Unsurprisingly, phenylalanine is the common backbone structure of these LAT1-specific radiotracers [54].

LAT1-specific PET radiotracers

1. [^{18}F]FBPA, [^{18}F]FBY, and [^{18}F]BBPA

The 4-borono-2-[^{18}F]fluoro-D,L-phenylalanine ([^{18}F]FBPA) was first synthesized in 1990, long before LAT1 was discovered [55]. [^{18}F]FBPA is a surrogate marker for tumor accumulation of 4-borono-D,L-phenylalanine (BPA). The boron atom (^{10}B) of BPA is the target compound of boron neutron capture therapy (BNCT), an irradiation technique for unresectable local malignancies. BPA is administered intravenously and ultimately accumulates within cancer cells. When bombarded by neutrons, ^{10}B atoms turn into radioactive ions radiating alpha particles, killing those cancer cells [56]. By radiolabeling BPA with ^{18}F, [^{18}F]FBPA PET study prior to BNCT can approximate the tumor-to-normal tissue (T/N) accumulation ratio of BPA (^{10}B). The T/N ratio was defined as the ratio of SUV_{max} obtained from tumor ROI to the SUV_{max} of the ROI of normal tissue surrounding the tumor lesion at the corresponding level on the PET/CT image slice. Several clinical trials showed that tumor lesions with a T/N ratio ≥ 2.5 are eligible for BNCT [57].

[^{18}F]FBPA is a product of ^{18}F radiolabeling either via [^{18}F]F_2 electrophilic substitution or [^{18}F]F^- nucleophilic substitution (typical yield in both approaches was similarly low, ±20-25%) [57]. A recent nucleophilic method produced non-carrier-added [^{18}F]FBPA with acceptable molar activity (56 ± 15 GBq/μmol) and suggested the potential to be automated for routine use [58]. It is worth noting that two isomers exist, L-[^{18}F]FBPA and D-[^{18}F]FBPA, depending on the radiolabeling starting material. Even though L-[^{18}F]FBPA has been chosen since early clinical use, the consideration was not LAT1 selectivity but the preference of melanoma for taking up L-enantiomers of amino acids [59]. On the other hand, D-amino acids are known for their lack of contribution to human amino acid metabolism. Indeed, D-[^{18}F]FBPA has scant accumulation in the brain, liver, spleen, pancreas, and bones [60]. Unfortunately, D-[^{18}F]FBPA is neither selective to LAT1 nor LAT2, nullifying its potential as a cancer-targeting PET radiotracer [61]. The term "[^{18}F]FBPA" in this review is meant for L-[^{18}F]FBPA.

[^{18}F]FBPA is claimed as LAT1-specific (K_m LAT1 = 197 μM, K_m ratio LAT2/LAT1=14), while BPA has much lower LAT1-specificity (K_m ratio LAT2/LAT1 = 4.3) [62]. In melanoma, [^{18}F]FBPA is involved in melanogenesis, and thus melanoma lesions have higher [^{18}F]FBPA uptake [57]. Adding the α-methyl group might improve the LAT1 selectivity (this tracer is still in early investigation) [63]. As a LAT1 substrate (subject to bi-directional transport), consequently, [^{18}F]FBPA tumor uptake is generally lower than PET radiotracers whose trapping mechanism within cancer cells, like [^{18}F]FDG. However, [^{18}F]FBPA tumor uptake is about similar to that of [^{11}C]MET [64]. A high-contrast image in [^{18}F]FBPA PET can be obtained earlier than the typical 60 min post-injection scan (**Figure 2**) [65]. [^{18}F]FBPA PET visualized thoracal and mediastinal malignant lesions with high contrast (**Figure 3A**) [66]. In benign lesions, [^{18}F]FBPA uptake was consistently low (SUV_{max} < 2), while [^{18}F]FDG uptake on the same lesions was higher (SUV_{max} > 5). More importantly, unlike [^{11}C]MET and [^{18}F]FDG, [^{18}F]FBPA does not accumulate in inflammatory tissues, including post-radiation necrotic lesions (**Figure 3B**) [67].

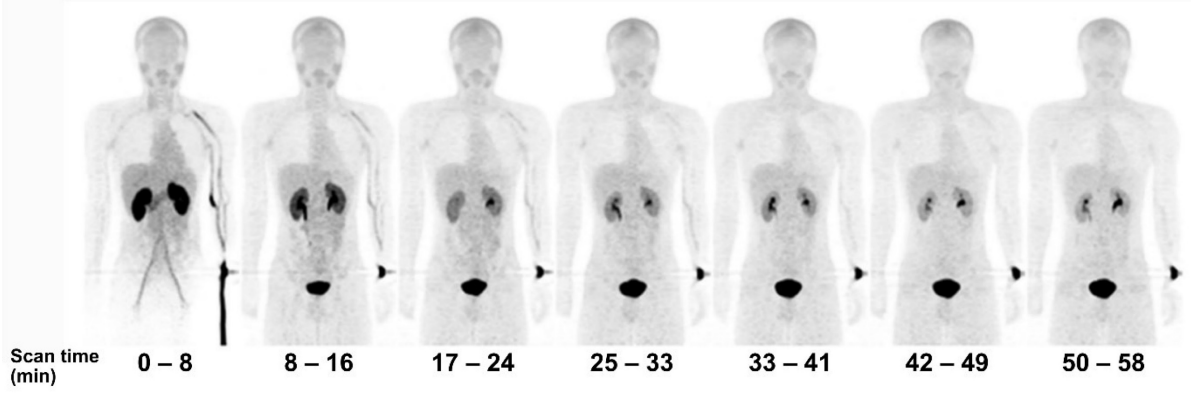

Figure 2. Serial PET mean intensity projection (MIP) images of [^{18}F]FBPA uptake in a healthy male. Kidney and pancreas uptake [^{18}F]FBPA rapidly cleared after injection. Pelvic kidney and bladder accumulation represent [^{18}F]FBPA excretion route. A high-contrast image can be obtained less than 1 hour after injection [65]. Adapted and reproduced with permission from Springer Nature. Copyright © 2016, The Japanese Society of Nuclear Medicine.

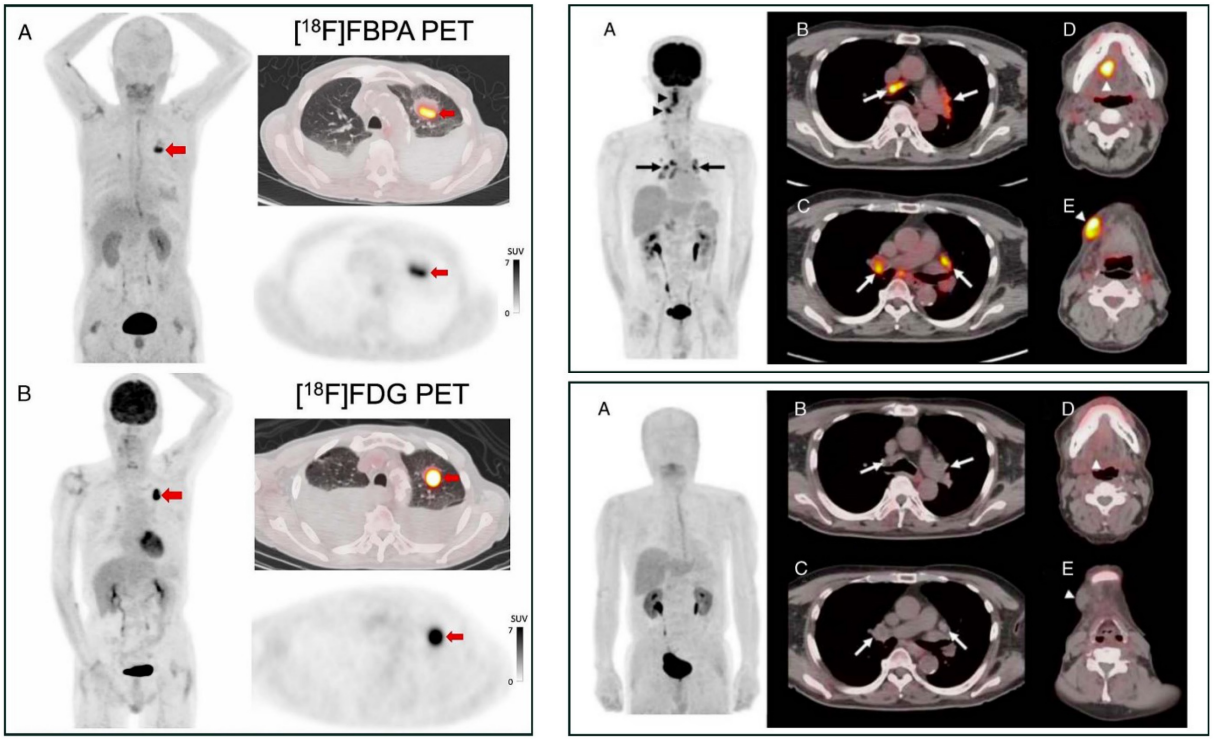

Figure 3. PET MIP and axial PET/CT image comparison between [18F]FBPA and [18F]FDG. **Left box:** A primary lung squamous cell carcinoma on a 71-year-old man (*red arrows*, [18F]FDG SUV_{max} 14.8 and [18F]FBPA SUV_{max} 7.2). Reproduced as is from [66]. Copyright © 2023, Copyright © 2023 The Author(s). Published by Wolters Kluwer Health, Inc. Originally published under Creative Commons Attribution-Non Commercial-No Derivatives License 4.0 (CCBY-NC-ND license). **Right boxes:** A tongue cancer and mediastinal sarcoidosis case in a 68-year-old man. The [18F]FDG PET images ***(upper box)*** and [18F]FBPA PET images ***(lower box)*** were taken ten and eleven days following high-dose brachytherapy for his tongue cancer, respectively. [18F]FDG PET images visualized active inflammation in his mediastinal sarcoidosis **(*upper box*, A–C, arrows)** and post-radiation inflammation **(*upper box*, D & E, arrowheads)**, while no [18F]FBPA uptake in the corresponding area of the mediastinum **(*lower box*, A–C, arrows)**, tongue, and submandibular region **(*lower box*, D & E, arrowheads)**. Reproduced as is from [67]. Copyright © 2020, Copyright © 2020 The Author(s). Published by Wolters Kluwer Health, Inc. Originally published under Creative Commons Attribution-Non Commercial-No Derivatives License 4.0 (CCBY-NC-ND license).

Head-to-head comparisons between [18F]FBPA and [18F]FDG PET involving enough patients are scarce. The SUV_{max} of [18F]FBPA and [18F]FDG are strongly correlated (n = 20, r = 0.72) for detecting head and neck cancer lesions [68]. However, their SUV_{max} correlation is weak (r = 0.48) as reported by a study (n = 82) involving head and neck squamous cell carcinoma and adenocarcinoma, adult and juvenile type sarcoma, malignant melanoma, and glioma) [69]. Interestingly, their intratumoral spatial distribution—measured by spatial parameters such as metabolic tumor volume (MTV)—is significantly dissimilar [70]. Even so, the absence or limited uptake of [18F]FBPA in benign lesions might be favorable for accurate cancer detection. In an exploratory study (n = 22 primary tumors, 55 metastatic lesions, and 11 benign lesions), Isohashi *et al.* found that the maximum standardized uptake volume (SUV_{max}) of [18F]FBPA is significantly higher for malignant lesions (5.1 ± 3.0 vs. 2.9 ± 0.6, p < 0.001), resulting in a potentially useful SUV_{max} cutoff at 3.24. In the same cohort, the SUV_{max} of [18F]FDG could not adequately discriminate malignant and benign lesions (SUV_{max} of 11.16 yields 90% sensitivity but only 39% specificity) [71]. However, in head and neck cancer cases, the PET parameters (SUV_{max}, SUV_{peak}) of [18F]FBPA were weakly correlated with LAT1 expression in tumor tissue specimens. Thus, sometimes [18F]FBPA uptake could not be reliably predicted BNCT treatment response [72].

Since June 2020, BNCT has been covered by national insurance in Japan for head and neck cancer. Thus, we may expect a wider use of [18F]FBPA PET. Meanwhile, Li *et al.* in China developed [18F]trifluoroboratetyrosine ([18F]FBY) as an alternative for BPA and [18F]FBPA (**Figure 1**) [73]. The reason was twofold: 1) *in vivo* deboronation of [18F]FBPA and 2) the distinct molecular structure between BPA and [18F]FBPA due to additional [18F] on the [18F]FBPA side chain. Both reasons contributed to the off-target irradiation during BNCT. The [18F]FBY unique radiolabeling approach replaces the amino acid carboxyl group with a negatively charged trifluoroborate group, allowing for quick radiolabeling (15 min) with favorable yield (~50%), radiochemical purity (~98%), and stability (4 h). [18F]FBY has molecular electrostatic potential, structure, and chemical characteristics similar to BPA and is metabolically more stable than BPA. Despite no information regarding LAT1 selectivity (in

comparison to LAT2), their *in vitro* and animal studies showed that boron concentration in tumor, muscle, and brain (therapeutic dose of FBY) is highly correlated with the mean SUV of [^{18}F]FBY in those regions. In humans, [^{18}F]FBY PET images presented a rapid kidney clearance, resulting in an extremely low background uptake at 60 min post-injection (**Figure 4**) [74]. Preliminary PET studies in primary brain tumors and brain metastases showed very promising potential of [^{18}F]FBY (T/N ratio at least 17.1 and 20.2, respectively [75] and better brain tumor lesions delineation than contrast-enhanced MRI [76]).

Li *et al*. continued their elaboration, and recently, they successfully synthesized [^{18}F]trifluoroborate-derived boronophenylalanine ([^{18}F]BBPA, **Figure 1**). The synthesis method was able to yield a stable and more than enough final [^{18}F]BBPA activity (± 1 Ci) for routine clinical PET imaging, and [^{18}F]BBPA was also stable and potentially a better BNCT compound since it has more boron atom and more tumor accumulation than BPA. [^{18}F]BBPA showed excellent pharmacokinetics and provided a clean background for high-contrast PET images. A limited clinical PET study showed that [^{18}F]BBPA may reach a T/N ratio in the brain up to 18, higher than most amino acid PET radiotracers [77]. However, more clinical data is warranted since [^{18}F]BBPA was also reported to accumulate in non-malignant tissue [78].

2. [^{18}F]FAMT and [^{18}F]FAMP

Among LAT1-specific amino acid-based PET radiotracers, 3-[^{18}F]fluoro-α-methyl-L-tyrosine ([^{18}F]FAMT, **Figure 1**) is probably the most extensively studied clinically for cancer within the last two decades [20]. The history of α-methyl-L-tyrosine compounds predates back to the 1980s when 3-[^{123}I]iodo-α-methyl-L-tyrosine ([^{123}I]IMT) SPECT was used as an alternative for [^{11}C]MET PET imaging of brain tumors [79]. It was revealed a decade later that [^{123}I]IMT is LAT1-selective [80], although it was also revealed that [^{123}I]IMT is a substrate for B^0 amino acid transporter system [81]. Compared to [^{11}C]MET PET for routine clinical use (^{11}C half-life is very short, and in the 1990s, PET camera was a rarity), [^{123}I]IMT SPECT was superior. However, the [^{123}I]IMT SPECT spatial image resolution is much lower than [^{11}C]MET PET, precluding the detection of small lesions [79].

In 1997, Tomiyoshi *et al.* at Gunma University developed a quick method (43 min) to synthesize [^{18}F]FAMT via [^{18}F]F_2 gas electrophilic substitution of α-methyl-L-tyrosine (radiochemical yield ± 20%, final radioactivity obtained was ± 1.5 GBq (40 mCi), limiting its use only to 2-4 patients) [82]. The imaging comparison in breast cancer xenografts with [^{11}C]MET, [^{99m}Tc]Tc-tetrofosmin, [^{99m}Tc]Tc-sestamibi, and [^{201}Tl]Tl-chloride showed that [^{18}F]FAMT had the highest tumor uptake, tumor-to muscle, and tumor to lung ratio [83]. Despite the low yield and low specific activity in each radiosynthesis, [^{18}F]FAMT has been routinely used in PET clinical studies until now. An alternative synthesis route for [^{18}F]FAMT was proposed years later via an automated, three-step, two-pot procedure of nucleophilic exchange reaction producing 32 ± 8% radiochemical yield (140 min) with a suitable amount of radioactivity for clinical use (> 20 GBq/mmol) [84]. The current automated synthesis could produce [^{18}F]FAMT up to 39 GBq/mmol specific activity [85]. One of the late-stage fluorination methods, which has been popular recently, has the potential to synthesize [^{18}F]FAMT with final radioactivity per batch of at least 10 GBq (270 mCi)) [86].

[^{18}F]FAMT is a highly specific LAT1-targeting radiopharmaceutical, thanks to its possession of α-methyl group (K_m LAT1 72.7 μM and no transport via LAT2) [29]. [^{18}F]FAMT is not metabolized nor incorporated into protein; thus, physiological uptake is negligible. Clinical [^{18}F]FAMT PET studies paired with histopathological data in various cases confirmed the presumption that LAT1 expression in normal tissues is very low. Except in the kidney, [^{18}F]FAMT physiological uptake in the brain, heart,

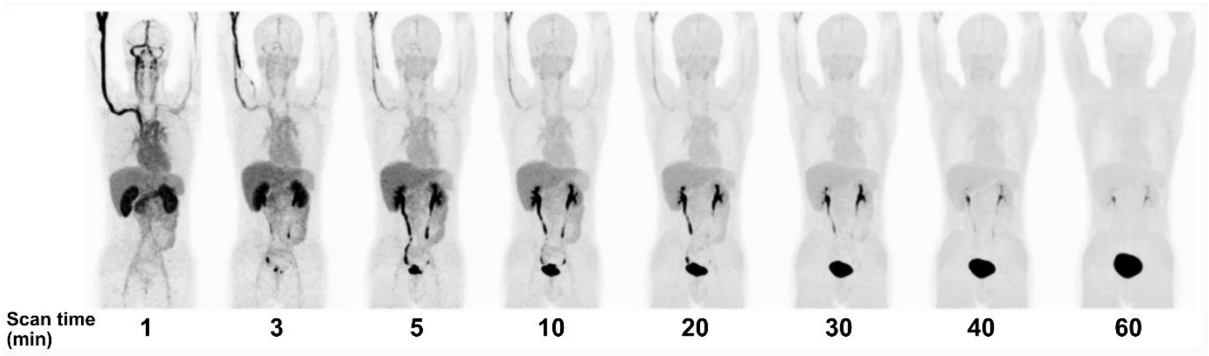

Figure 4. PET MIP images over time after [^{18}F]FBY administration in a healthy volunteer. Adapted with permission from [74]. Copyright © 2021, The Author(s), under exclusive license to Springer-Verlag GmbH, DE, part of Springer Nature.

lung, liver, and bone marrow is significantly less than [^{18}F]FDG (**Figure 5**). Most importantly, [^{18}F]FAMT uptake in muscle is as low as [^{18}F]FDG [50]. Thus, even though the absolute lesion uptake of [^{18}F]FAMT is lower than that of [^{18}F]FDG, high-contrast images can be obtained due to low background activity. [^{18}F]FAMT enantiomeric tracer, D-[^{18}F]FAMT, has been predicted to have lower renal retention since D-amino acid is rarely involved in human metabolism. The presumption was proven true; however, D-[^{18}F]FAMT has even lower absolute tumor uptake than L-[^{18}F]FAMT, preventing this enantiomeric tracer from being further explored [87].

[^{18}F]FAMT uptake in inflammations is also lower than that of [^{18}F]FDG, as confirmed in preclinical [88, 89] and clinical studies [90, 91]. A dynamic study in animal tumor models showed that both total distribution volumes of [^{18}F]FBPA and [^{18}F]FAMT within the tumor represent the tumor expression levels of LAT1 and are not influenced by the tumor blood flow [85]. This finding showed [^{18}F]FBPA and [^{18}F]FAMT potential for evaluating the LAT1 expressions in hypoxic cancer lesions or those with low vascular density. Unfortunately, direct clinical comparison with other amino acid PET radiotracers is lacking. The typical highest major organ uptake of other amino acid PET radiotracers compared to that of [^{18}F]FAMT was summarized in **Table 1**.

Head-to-head diagnostic accuracy tests comparing [^{18}F]FAMT and [^{18}F]FDG for malignancy detection suggested that they have equal sensitivity, yet [^{18}F]FAMT has higher tumor specificity [51]. [^{18}F]FAMT PET/CT has been clinically useful as a diagnostic and prognostic tool in various cancer types, e.g., glioma [92], lung [93], esophageal [94], and oral cancers [95]. Clinical [^{18}F]FAMT PET studies on various cancers (in comparison to [^{18}F]FDG) over the last two decades are summarized in **Table S2**.

The high [^{18}F]FAMT radioactivity in the kidney is not only due to the excretory route (**Figure 5**) [50]. The 3-fluorine and 4-hydroxyl group of [^{18}F]FAMT render it recognized as a substrate by OAT1, an organic anion transporter on renal tubular epithelial cells, facilitating prolonged kidney retention [96]. Administering OAT1 inhibitors (e.g., probenecid) before [^{18}F]FAMT injection has been proven efficient in animal models to delay [^{18}F]FAMT blood clearance and thus increase tumor uptake [97].

The [^{18}F]FAMT absolute tumor uptake is relatively low compared to that of [^{18}F]FDG due to the LAT1 bi-directional transport, resulting in fast clearance from the tumor. This quick tumor washout may lead to false negative findings. However, it is important to note that in all [^{18}F]FAMT PET clinical studies, a scan is obtained about 60 min post-injection. Therefore, a dynamic [^{18}F]FAMT PET study is essential to determine the optimal scan time. A dynamic PET study in mice showed that [^{18}F]FAMT can rule out granuloma from gliomas in which static images failed to do so [89]. However, glioma uptake patterns might vary for different grades since low-grade glioma metabolizes fewer amino acids and expresses less LAT1 [98]. Dynamic [^{18}F]FET PET studies in glioma provided insights for scan protocol adjustment, thus included in the current guidelines [5]. If a dynamic PET study is not feasible, an early static scan at 5–15 min post-injection is more accurate for differentiating glioma grades than the 20–40 static scan [99]. Unfortunately, such clinical dynamic PET studies are currently lacking for [^{18}F]FAMT.

The limitations in [^{18}F]FAMT synthesis and the short half-life of ^{18}F inspiring the use of a longer half-life positron emitters, ^{76}Br (mean energy 650 keV, $t_{1/2}$ = 16.2 h) and ^{77}Br (mean energy 336 keV, $t_{1/2}$ = 57 h) for α-methyl-L-tyrosine radiolabeling. Their relatively long half-life allows larger-scale radiosynthesis by a nuclear facility for delivery to regional hospitals. The initial study revealed that 3-[$^{76/77}$Br]BAMT *in vivo* is metabolized over time and debrominated, resulting in slow blood clearance and

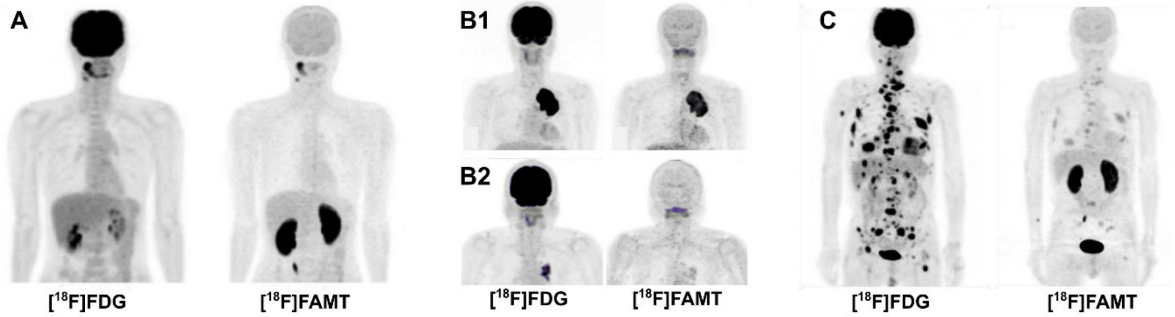

Figure 5. Comparison of PET MIP images of [^{18}F]FDG and [^{18}F]FAMT in malignancies, 60 min post-administration (*author's data*). **(A)** A 40-year-old man with oral squamous cell carcinoma. [^{18}F]FAMT uptake in the brain and other major organs is minimal, while kidney uptake is prominent. **(B1, B2)** [^{18}F]FAMT provided a prognostic tool for overall survival in non-small cell lung cancer patients. A 60-year-old man (stage IIIB, T4N0M0) with high [^{18}F]FAMT tumor uptake had survived for only 122 days **(B1)**, while a 72-year-old man (stage IIIA, T2N2M0) with faint [^{18}F]FAMT tumor uptake indicating less aggressive tumor, survived until 1,875 days later **(B2)**. **(C)** A 73-year-old man with metastatic large-cell neuroendocrine lung carcinoma with faint [^{18}F]FAMT uptake in all lesions.

high accumulation of free bromine in normal organs [100]. In a subsequent study, ^{76}Br or ^{77}Br were radiolabeled onto L-α-methyl-phenylalanine, which lacks the phenolic hydroxyl group compared to L-α-methyl-tyrosine (**Figure 1**). The 2-[$^{76/77}$Br]bromo-α-methyl-L-phenylalanine (2-[$^{76/77}$Br]BAMP) demonstrated preferable *in vivo* stability and faster blood clearance than 3-[$^{76/77}$Br]BAMT and even [^{18}F]FAMT. In particular, 2-[$^{76/77}$Br]BAMP displayed a much lower kidney accumulation at 60 min post-injection than 3-[$^{76/77}$Br]BAMT and [^{18}F]FAMT. Interestingly, the tumor-to-muscle uptake ratio of 2-[$^{76/77}$Br]BAMP continued increasing from 1 to 3 h post-injection due to quick muscle clearance [101].

The ideal characteristic of 2-[$^{76/77}$Br]BAMP subsequently reignited the idea of ^{18}F radiolabeling and drove the development of [^{18}F]fluoro-α-methyl-L-phenylalanine ([^{18}F]FAMP, **Figure 1**). Among regioisomer and stereoisomer of α-methyl-phenylalanine tested, 2-[^{18}F]fluoro-α-methyl-L-phenylalanine ([^{18}F]FAMP) featured high tumor uptake via LAT1 (higher than [^{18}F]FAMT) and low kidney accumulation (significantly less than [^{18}F]FAMT). Similar to the 2-[$^{76/77}$Br]BAMP tumor uptake pattern, [^{18}F]FAMP clearly visualized orthotopic bladder tumors at 3 h post-injection because of quick muscle clearance [102]. Fascinatingly, the *in vivo* stability, pharmacokinetics, and LAT1 tumor uptake of 2-α-methyl-L-phenylalanine analog remains unaffected when α-particle emitter astatine-211 (^{211}At) is integrated to construct the therapeutic analog 2-[^{211}At]-astato-α-methyl-L-phenylalanine ([^{211}At]AAMP) [103]. Again, similar to [^{18}F]FAMT, probenecid loading also reduces [^{211}At]AAMP kidney uptake and enhances tumor accumulation, improving its therapeutic effect in murine tumor models [104].

The direct electrophilic substitution synthesis route of [^{18}F]FAMP produces low radiochemical yield (20-30%) and specific activity (2-3 MBq/μmol) [105]. However, a proposed late-stage fluorination method using *N*-pivaloyl chloride-protected (mesityl)(aryl) iodonium salt precursor could obtain [^{18}F]FAMP within 120 min (radiochemical yield 21.4%, radiochemical purity >95%, and specific activity >37 GBq/μmol) [86]. Thus, a large-scale clinical trial is awaited to pave the way for [^{18}F]FAMP clinical use.

3. [^{18}F]FIMP

Another research group in Japan developed an α-methyl-L-phenylalanine analog based on screening using human LAT1 and LAT2 overexpressed cell lines. They found that *(S)*-2-amino-3-[3-(2-[^{18}F]-fluoroethoxy)-4-iodophenyl]-2-methylpropanoic acid ([^{18}F]FIMP, **Figure 1**) was among the LAT1 high-affinity substrate (IC_{50} 88.5 ± 13.5 μM). The ^{18}F radiolabeling via nucleophilic substitution method produced [^{18}F]FIMP with >98% radiochemical purity and high specific activity up to 122 GBq/μmol [106].

In a study of animal tumor and inflammation model, [^{18}F]FIMP was not metabolized into protein; thus, [^{18}F]FIMP was stable and excreted almost intact in urine. [^{18}F]FIMP has similar tumor uptake to [^{18}F]FDG, while uptake in inflamed lesions was significantly less. However, [^{18}F]FIMP muscle uptake was higher than [^{18}F]FDG; thus, the [^{18}F]FIMP tumor-to-muscle ratio was less than [^{18}F]FDG. Compared to [^{18}F]FET, inflammation uptake of [^{18}F]FIMP was higher. Nevertheless, since [^{18}F]FIMP has higher tumor uptake and less muscle uptake than [^{18}F]FET, [^{18}F]FIMP PET image has significantly better contrast [106]. A further investigation detailing [^{18}F]FIMP specificity toward other amino acid transporters revealed that [^{18}F]FIMP is also a substrate of $ATB^{0,+}$ (SLC6A14), just like [^{18}F]FET [107]. However, $ATB^{0,+}$ (SLC6A14) protein expression is too low to be detected in healthy tissues [108]. Thus, the extended muscle uptake of [^{18}F]FIMP is likely due to its pharmacokinetics rather than transport by $ATB^{0,+}$. The $ATB^{0,+}$ is significantly increased in some cancers (pancreatic, cervical, colon, and estrogen-positive breast cancers); thus [^{18}F]FIMP perhaps has potential for cancer detection via $ATB^{0,+}$-targeting. However, this subtopic is beyond the scope of the current review.

The first-in-human investigation of [^{18}F]FIMP PET has been done recently in healthy volunteers and brain tumor patients in comparison with [^{11}C]MET and [^{18}F]FDG. [^{18}F]FIMP rapidly cleared from the blood, resulting in very low background activity 1-hour post-injection. As expected, a clear margin of glioblastoma (grade IV glioma) can be demonstrated with higher contrast than that with [^{11}C]MET and [^{18}F]FDG [109]. Due to their low brain physiological uptake, amino acid-based PET radiotracers have long been expected to replace [^{18}F]FDG in various scenarios in neurooncology cases [27, 110]. One of their fundamental problems is their affinity toward LAT2. LAT2 is expressed on the plasma membrane of neuronal axons in the cerebral cortex, choroid plexus, subfornical organ, and hypothalamus [111]. In inflammation-related neurooncology cases like radiation necrosis, amino acid PET radiotracer should also be able to discriminate cancer lesions from inflamed tissues. Current evidence favors amino acid PET radiotracers ([^{11}C]MET, [^{18}F]FET, and [^{18}F]DOPA) for post-radiotherapy cases; however, they are inconclusive in terms of which PET radiotracers are the best [112-114]. Thus, it is interesting to watch the diagnostic performance of [^{18}F]FIMP PET in

neurooncology cases against the established PET radiotracer [^{18}F]FET [5], especially considering that [^{18}F]FIMP is less prone to post-radiotherapy inflammation [115].

4. [^{18}F]FELP

The [^{18}F]FET (*O*-[^{18}F]fluoroethyl-L-tyrosine) is arguably one of the most popular amino acid-based PET radiotracer. Even though [^{18}F]FET is not LAT1-specific, [^{18}F]FET has an efficient radiosynthesis route, allowing a large quantity of production for routine clinical use and distribution to surrounding hospitals [5]. Inspired by [^{18}F]FET, a *para*-fluoroethyl of alkylated phenylalanine, *p*-(2-[^{18}F]fluoroethyl)-L-phenylalanine (*(S)*-4-[^{18}F]FELP) was successfully synthesized (>95% radiochemical purity, up to 37% yield, and up to 69 GBq/μmol specific activity within 90 min) and showed LAT1-selective uptake in animal tumor models [116]. Recently, the *ortho*- and *meta*-substitution versions of fluoroethyl phenylalanine and their enantiomers were studied. Among these analogs, 2-[^{18}F]-2-fluoroethyl-L-phenylalanine (*(S)*-2-[^{18}F]FELP or [^{18}F]FELP, **Figure 1**) was the most LAT1-specific (K_m 8.72—16.36 μM, in competition with JPH203, a LAT1-specific and potent inhibitor).

Imaging comparison between [^{18}F]FELP and [^{18}F]FET in an orthotopic glioblastoma rat model demonstrated comparable SUV and tumor-to-background ratios (**Figure 6**) [117]. In a similar animal model, [^{18}F]FELP also showed its potential to discriminate glioblastoma lesions from radiation necrosis, as well as [^{18}F]FET [118]. Until now, [^{18}F]FELP PET studies in humans have not yet been reported.

5. LAT1 inhibitor-based PET radiotracers

A high-affinity, non-transportable LAT1-specific blocker has been successfully synthesized based on their structure-activity relationship [119]. This LAT1 inhibitor, JPH203 (nanvuranlat; IC_{50} 0.14 μM, no transport via LAT2) [120], underwent a series of *in vitro* and *in vivo* studies confirming its potential for a *pan-cancer* therapeutic agent [26]. A Japanese pharma company conducted a phase III clinical trial of JPH203 and investigated several variants of LAT1 inhibitors. They also investigated NKO-028 and NKO-035, two amino acid derivative LAT1-selective substrates, as prospective PET radiotracers for solid tumors [121].

[^{18}F]NKO-028 and [^{18}F]NKO-035 were claimed to be LAT1-specific with high affinity. [^{18}F]NKO-028 synthesis took 80 min with a 30% radiochemical yield, while automated synthesis could obtain [^{18}F]NKO-035 with 1,000 GBq/μmol specific activity and >99% radiochemical purity (50:50 enantiomeric mixture of L- and D-form) in 68 min [122]. Both PET radiotracers have no specific accumulation in major organs. High [^{18}F]NKO-028 accumulation in the spleen, kidney, and other organs was decreased rapidly after administration [123]. On the other hand, when [^{18}F]NKO-035 was tested in rat inflammation models, physiological uptake remained observed on the kidneys and pancreas at 60 min post-administration. Nevertheless, [^{18}F]NKO-035 is relatively stable *in vivo* (90% unchanged at 75 min) and demonstrated low uptakes on inflammatory lesions [124].

A human dosimetry study confirmed that [^{18}F]NKO-035 has minimal accumulation in normal tissues except in the bladder, kidneys, and urinary tracts. A typical [^{18}F]NKO-035 injection dose of ±221 MBq exposes each patient to an effective dose of 4.4 mSv (including a CT dose of 2.3 mSv) [125]. For comparison, almost half of the effective dose in a whole-body [^{18}F]FDG PET/CT scan (±244 MBq dose of [^{18}F]FDG) generated 4.2 mSv effective dose, without CT dose included [126]. Another human dosimetry study designed to calculate the 2 Gy equieffective dose (EQD2(α/β)) parameter using [^{18}F]NKO-035 implies the possibility of developing NKO-035 as a LAT1-targeting α-particle emitter therapy using ^{211}At. The dynamic PET acquisition of [^{18}F]NKO-035 demonstrated very low background

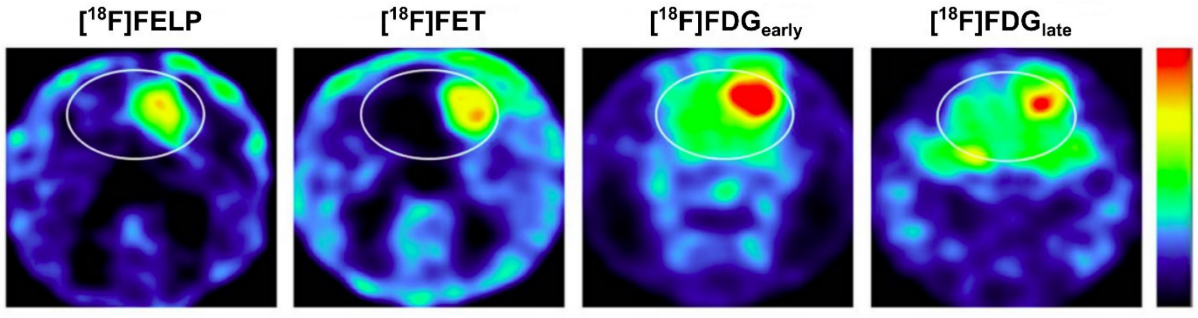

Figure 6. [^{18}F]FELP depicted a tumor uptake level similar to [^{18}F]FET in Micro PET images of orthotopic glioblastoma rat models, with less background uptake (both images were taken 100 min post-injection). A later [^{18}F]FDG image (240 min post-injection) demonstrated less normal brain tissue uptake than the early image, but those uptakes remained higher than that on [^{18}F]FELP and [^{18}F]FET images. Adapted from [117].

uptake at 60 min post-injection, potentially delivering images with higher contrast than [^{18}F]FDG PET [127]. It is very compelling to find out whether the slow kidney clearance of [^{18}F]NKO-035 is also facilitated by a similar mechanism to [^{18}F]FAMT. If so, a similar approach to inhibit OAT1 can be implemented. Clinical translation of [^{18}F]NKO-035 is ongoing; thus, we are excited to see its diagnostic performance against [^{18}F]FDG and other amino acid-based PET radiotracers in various cancers [128].

Several prospective LAT1 inhibitors have been shortlisted from a virtual screening of large databases based on dynamic pharmacophores generated from molecular dynamic simulations. In particular, two of the 13 compounds demonstrated a highly potent LAT1 inhibition in a competitive *in vitro* assay against L-histidine, the LAT1 natural amino acid substrate with the highest affinity [129]. Developing these potent LAT1 inhibitors as PET radiotracers in future studies might be promising.

Conclusions and Perspectives

LAT1 is a *pan-cancer* molecular target promising for cancer diagnosis. LAT1 overexpression in cancer is also prognostic for survival and, thus, may serve as a monitoring biomarker of therapeutic responses. Clinical evidence showed that LAT1 targeting PET imaging can discriminate malignant tissue from benign components in a heterogeneous tumor mass. The lack of LAT1 expression in non-cancer pathologies (e.g., benign tumors, inflammatory tissues, radiation necrosis) allows these PET radiotracers to delineate the actual borders of malignant tissue with high accuracy. Since the dynamics of LAT1 expression highly correlate with the behavior of cancer cells, LAT1-specific PET radiotracers would firmly stand on a wide spectrum of cancer management, from early detection, differential diagnosis, and therapy response monitoring to long-term prognostication. Therefore, LAT1-specific PET radiotracers may compensate for the limitations of the current standard oncologic PET radiotracer. Major advantages and known challenges of LAT1 targeting using PET radiotracers discussed in this review are summarized in **Table 2**.

Table 2. LAT1-specific PET radiopharmaceuticals: Advantages and challenges

LAT1-specific PET radio-pharmaceuticals	Advantages as a LAT1-targeting radiotracer	Challenges
[^{18}F]FBPA	Clinically used to predict boron accumulation in tumors before BNCT Suitable for malignant melanoma due to prolonged retention No uptake in inflammation and benign lesions. Typical T/N ratio for malignancy is >2.5 High contrast whole body image might be obtained as early as 20–30 min p.i.	Limited availability (Japan, Finland, China, United States, Taiwan) Limited specific activity using the current radiosynthesis method (a new synthesis method is available) *In vivo* deboronation Poor water solubility (can be solved with the addition of fructose)
[^{18}F]FBY	Potentially a better predictor for boron accumulation before BNCT Excellent stability against defluorination or deboronation T/N ratio ranges from 2.3 to 24.5 High contrast whole body image might be obtained as early as 30–40 min p.i.	Limited availability (China) Need more clinical data
[^{18}F]BBPA	Potentially a better predictor for boron accumulation before BNCT Can be obtained in Curie-level amount Excellent stability against defluorination or deboronation Mean T/N ratio in the brain = 18.7 High contrast whole body image might be obtained as early as 30–40 min p.i.	Uptake was found in non-malignant lesions Limited availability (China) Need more clinical data
[^{18}F]FAMT	Clinically proven as a diagnostic and prognostic tool No uptake in inflammation and benign lesions High contrast whole body image might be obtained as early as 40–60 min p.i.	Limited availability (Japan) Limited specific activity using the current radiosynthesis method (a new synthesis method is available) High kidney retention (can be reduced with probenecid preloading)
[^{18}F]FAMP	Similar to [^{18}F]FAMT regarding normal tissue distribution, yet higher tumor uptake and lower kidney retention	Limited availability (Japan) Limited specific activity using the current radiosynthesis method (a new synthesis method is available) High pancreas uptake No clinical data is available yet
[^{18}F]FIMP	High contrast whole body image might be obtained at around 60 min p.i. No uptake in radiation necrosis (inflammation)	Limited availability (Japan) Very limited clinical data
[^{18}F]FELP	No uptake in radiation necrosis and inflammatory tissues	Limited availability (Belgium) No clinical data is available yet
[^{18}F]NKO-035	A high contrast whole body image might be obtained at around 60 min p.i. Low uptake in inflammatory tissue	Limited availability (Japan) Relatively high kidney retention Very limited clinical data

Note: **p.i.** post injection

As previously mentioned, most PET radiopharmaceuticals claimed to be LAT1-specific are LAT1 substrates, hence prone to washout due to LAT1 efflux. Even though the absolute tumor uptake of the current LAT1-specific PET radiotracers has a lower quantity than [^{18}F]FDG, the lack of LAT1 expression in the plasma membrane of normal tissues allows tumor accumulation of these PET radiotracers to generate clinical PET images with a relatively high tumor-to-background (or T/N) ratio (see **Table S1**). In the future, the development of LAT1-specific PET radiotracers equipped with favorable characteristics such as high affinity, good biodistribution, early uptake, and faster blood clearance is warranted. A non-transportable LAT1 inhibitor may also be a favorable characteristic; however, tumor uptake can be much improved if a LAT1-specific PET radiotracer could be internalized into the cytoplasm and retained there without the possibility of being effluxed. The detailed structure of LAT1, including the binding pocket, gating mechanism, and substrate/inhibitor preferences, should be the basis for further development of LAT1-specific PET radiopharmaceuticals.

In conclusion, several LAT1-specific PET radiotracers are in the final stages of preclinical studies or even phase II/III clinical trials. Once these LAT1-specific PET radiotracers are approved for clinical use by the government regulatory bodies, we may expect improvement in multiple aspects of cancer management.

Abbreviations

ASCT2: Alanine, Serine, Cysteine Transporter 2; BNCT: boron neutron capture therapy; [$^{76/77}$Br]BAMP: 2-[$^{76/77}$Br]bromo-α-methyl-L-phenylalanine; [$^{76/77}$Br] BAMT: 3-[$^{76/77}$Br]bromo-α-methyl-L-tyrosine; [^{11}C] MET: L-[*methyl*-^{11}C]methionine or 2-amino-4-[^{11}C] methylsulfanyl-butanoic acid; [^{18}F]FAMP: 2-[^{18}F] fluoro-α-methyl-L-phenylalanine; [^{18}F]FAMT: 3-[^{18}F] fluoro-α-methyl-L-tyrosine; [^{18}F]FBPA: 4-borono-2-[^{18}F]fluoro-D,L-phenylalanine; [^{18}F]FBY: [^{18}F]fluoro-boronotyrosine; [^{18}F]FDG: [^{18}F]fluorodeoxyglucose or 2-deoxy-2-[^{18}F]fluoro-D-glucose; [^{18}F]FDOPA: [^{18}F] fluorodopa or 3,4-dihydroxy-6-[^{18}F]fluoro-L-phenylalanine; [^{18}F]FELP: 2-[^{18}F]-2-fluoroethyl-L-phenylalanine; [^{18}F]FET: *O*-[^{18}F]fluoroethyl-L-tyrosine; [^{18}F]FIMP: *(S)*-2-amino-3-[3-(2-[^{18}F]-fluoroethoxy)-4-iodophenyl]-2-methylpropanoic acid; [^{123}I]IMT: 3-[^{123}I]iodo-α-methyl-L-tyrosine; LAT1: L-type amino acid transporter 1; MIP: mean intensity projection; PET: positron emission tomography; SUV_{max}: maximum standardized uptake volume; SUV_{peak}: peak standardized uptake volume.

Supplementary Material

Supplementary tables.
https://www.thno.org/v15p1864s1.pdf

Acknowledgments

Funding

This research was funded by the Directorate for Research and Community Service, Universitas Padjadjaran, grant number 1733/UN6.3.1/LT/2020.

Universitas Padjadjaran funded the article processing charges.

Author contributions

Conceptualization, A.A.;
Data curation, H.H., H.A.H., K.E, and A.A.;
Writing—original draft preparation, A.A.;
Writing—review and editing, A.A, H.H., H.A.H., K.E., Y.T., and A.H.S.K.;
Visualization, A.A.;
Supervision, A.H.S.K.;
Funding acquisition, A.H.S.K.
All authors have read and agreed to the published version of the manuscript.

Competing Interests

The authors are former (A.A., H.H., K.E.) and current (Y.T.) educational staff at the academic institution where the [^{18}F]FAMT is developed. The remaining authors (H.A.H., A.H.S.K.) declare that they have no known competing financial interests or personal relationships that could have appeared to influence the work reported in this paper. The funder (Universitas Padjadjaran) had no role in the study's design, data collection, analysis, interpretation, manuscript writing, or decision to publish the results.

References

1. Crișan G, Moldovean-Cioroianu NS, Timaru D-G, Andrieș G, Căinap C, Chiș V. Radiopharmaceuticals for PET and SPECT Imaging: A Literature Review over the Last Decade. Int J Mol Sci. 2022; 23: 5023.
2. Boellaard R, Delgado-Bolton RC, Oyen WJ, Giammarile F, Tatsch K, Eschner W, et al. FDG PET/CT: EANM procedure guidelines for tumour imaging: version 2.0. Eur J Nucl Med Mol Imaging. 2015; 42: 328-54.
3. Vali R, Alessio A, Balza R, Borgwardt L, Bar-Sever Z, Czachowski M, et al. SNMMI procedure standard/EANM practice guideline on pediatric ^{18}F-FDG PET/CT for oncology 1.0. J Nucl Med. 2021; 62: 99-110.
4. Delgado-Bolton RC, Aide N, Colletti PM, Ferrero A, Paez D, Skanjeti A, et al. EANM guideline on the role of 2-[^{18}F]FDG PET/CT in diagnosis, staging, prognostic value, therapy assessment and restaging of ovarian cancer, endorsed by the American College of Nuclear Medicine (ACNM), the Society of Nuclear Medicine and Molecular Imaging (SNMMI) and the International Atomic Energy Agency (IAEA). Eur J Nucl Med Mol Imaging. 2021; 48: 3286-302.
5. Law I, Albert NL, Arbizu J, Boellaard R, Drzezga A, Galldiks N, et al. Joint EANM/EANO/RANO practice guidelines/SNMMI procedure standards for imaging of gliomas using PET with radiolabelled amino acids and [^{18}F] FDG: version 1.0. Eur J Nucl Med Mol Imaging. 2019; 46: 540-57.
6. Piccardo A, Albert NL, Borgwardt L, Fahey FH, Hargrave D, Galldiks N, et al. Joint EANM/SIOPE/RAPNO practice guidelines/SNMMI

procedure standards for imaging of paediatric gliomas using PET with radiolabelled amino acids and [18F]FDG: version 1.0. Eur J Nucl Med Mol Imaging. 2022; 49: 3852-69.
7. Sarikaya I. Biology of cancer and PET imaging: Pictorial review. J Nucl Med Tech. 2022; 50: 81-9.
8. Cutler CS, Bailey E, Kumar V, Schwarz SW, Bom HS, Hatazawa J, et al. Global Issues of Radiopharmaceutical Access and Availability: A Nuclear Medicine Global Initiative Project. J Nucl Med. 2021; 62: 422-30.
9. Kratochwil C, Flechsig P, Lindner T, Abderrahim L, Altmann A, Mier W, et al. 68Ga-FAPI PET/CT: Tracer Uptake in 28 Different Kinds of Cancer. J Nucl Med. 2019; 60: 801-5.
10. Mori Y, Dendl K, Cardinale J, Kratochwil C, Giesel FL, Haberkorn U. FAPI PET: Fibroblast Activation Protein Inhibitor Use in Oncologic and Nononcologic Disease. Radiology. 2023; 306: e220749.
11. Chen X, Wang S, Lai Y, Wang G, Wei M, Jin X, et al. Fibroblast Activation Protein and Glycolysis in Lymphoma Diagnosis: Comparison of 68Ga-FAPI PET/CT and 18F-FDG PET/CT. J Nucl Med. 2023; 64: 1399-405.
12. Elboga U, Sahin E, Cayirli YB, Okuyan M, Aktas G, Haydaroglu Sahin H, et al. Comparison of [68Ga]-FAPI PET/CT and [18F]-FDG PET/CT in Multiple Myeloma: Clinical Experience. Tomography. 2022; 8: 293-302.
13. Broer S. Amino Acid Transporters as Targets for Cancer Therapy: Why, Where, When, and How. Int J Mol Sci. 2020; 21: 6156.
14. Lee ST, Burvenich I, Scott AM. Novel Target Selection for Nuclear Medicine Studies. Semin Nucl Med. 2019; 49: 357-68.
15. Rong J, Haider A, Jeppesen TE, Josephson L, Liang SH. Radiochemistry for positron emission tomography. Nat Comm. 2023; 14: 3257.
16. Jager PL, Vaalburg W, Pruim J, de Vries EG, Langen K-J, Piers DA. Radiolabeled amino acids: Basic aspects and clinical applications in oncology. J Nucl Med. 2001; 42: 432-45.
17. Bray F, Laversanne M, Sung H, Ferlay J, Siegel RL, Soerjomataram I, et al. Global cancer statistics 2022: GLOBOCAN estimates of incidence and mortality worldwide for 36 cancers in 185 countries. CA: Cancer J Clin. 2024; 74: 229-63.
18. Kandasamy P, Gyimesi G, Kanai Y, Hediger MA. Amino acid transporters revisited: New views in health and disease. Trends Biochem Sci. 2018; 43: 752-89.
19. Nakaya M, Xiao Y, Zhou X, Chang J-H, Chang M, Cheng X, et al. Inflammatory T cell responses rely on amino acid transporter ASCT2 facilitation of glutamine uptake and mTORC1 kinase activation. Immunity. 2014; 40: 692-705.
20. Kanai Y. Amino acid transporter LAT1 (SLC7A5) as a molecular target for cancer diagnosis and therapeutics. Pharmacol Ther. 2022; 230: 107964.
21. Scalise M, Galluccio M, Console L, Pochini L, Indiveri C. The human SLC7A5 (LAT1): The intriguing histidine/large neutral amino acid transporter and its relevance to human health. Front Chem. 2018; 6: 243.
22. Fan X, Ross DD, Arakawa H, Ganapathy V, Tamai I, Nakanishi T. Impact of system L amino acid transporter 1 (LAT1) on proliferation of human ovarian cancer cells: a possible target for combination therapy with anti-proliferative aminopeptidase inhibitors. Biochem Pharmacol. 2010; 80: 811-8.
23. Scalise M, Console L, Rovella F, Galluccio M, Pochini L, Indiveri C. Membrane transporters for amino acids as players of cancer metabolic rewiring. Cells. 2020; 9: 2028.
24. Jigjidkhorloo N, Kanekura K, Matsubayashi J, Akahane D, Fujita K, Oikawa K, et al. Expression of L-type amino acid transporter 1 is a poor prognostic factor for Non-Hodgkin's lymphoma. Sci Rep. 2021; 11: 21638.
25. Lopes C, Pereira C, Medeiros R. ASCT2 and LAT1 Contribution to the Hallmarks of Cancer: From a Molecular Perspective to Clinical Translation. Cancers. 2021; 13: 203.
26. Achmad A, Lestari S, Holik HA, Rahayu D, Bashari MH, Faried A, et al. Highly Specific L-Type Amino Acid Transporter 1 Inhibition by JPH203 as a Potential Pan-Cancer Treatment. Processes. 2021; 9: 1170.
27. Treglia G, Muoio B. Evidence-based PET for brain tumours. Evidence-based Positron Emission Tomography: Summary of Recent Meta-analyses on PET: Springer, Cham; 2020. p. 25-33.
28. Napolitano L, Galluccio M, Scalise M, Parravicini C, Palazzolo L, Eberini I, et al. Novel insights into the transport mechanism of the human amino acid transporter LAT1 (SLC7A5). Probing critical residues for substrate translocation. Biochim Biophys Acta. 2017; 1861: 727-36.
29. Wei L, Tominaga H, Ohgaki R, Wiriyasermkul P, Hagiwara K, Okuda S, et al. Specific transport of 3-fluoro-l-α-methyl-tyrosine by LAT1 explains its specificity to malignant tumors in imaging. Cancer Sci. 2016; 107: 347-52.
30. Kong F-L, J Yang D. Amino acid transporter-targeted radiotracers for molecular imaging in oncology. Curr Med Chem. 2012; 19: 3271-81.
31. Haubner R. PET radiopharmaceuticals in radiation treatment planning - Synthesis and biological characteristics. Radiother Oncol. 2010; 96: 280-7.
32. Zhao C, Zhang Y, Wang J. A meta-analysis on the diagnostic performance of 18F-FDG and 11C-methionine PET for differentiating brain tumors. AJNR Am J Neuroradiol. 2014; 35: 1058-65.
33. Xu W, Gao L, Shao A, Zheng J, Zhang J. The performance of 11C-Methionine PET in the differential diagnosis of glioma recurrence. Oncotarget. 2017; 8: 91030.
34. Zwart PLd, Dijken BRv, Holtman GA, Stormezand GN, Dierckx RA, Laar PJv, et al. Diagnostic Accuracy of PET Tracers for the Differentiation of Tumor Progression from Treatment-Related Changes in High-Grade Glioma: A Systematic Review and Metaanalysis. J Nucl Med. 2020; 61: 498-504.
35. Caldarella C, Treglia G, Isgrò MA, Giordano A. Diagnostic performance of positron emission tomography using 11C-methionine in patients with suspected parathyroid adenoma: a meta-analysis. Endocrine. 2013; 43: 78-83.
36. Filippi L, Frantellizzi V, Bartoletti P, Vincentis GD, Schillaci O, Evangelista L. Head-to-Head Comparison between FDG and 11C-Methionine in Multiple Myeloma: A Systematic Review. Diagnostics. 2023; 13: 2009.
37. Huo H, Shen S, Zhang L, Yang F, Li Y. The diagnostic performance of [18F]FET PET/MRI versus [18F]FDG PET/MRI for recurrent glioma: A systematic review and meta-analysis. Clin Transl Imaging. 2023; 11: 285-95.
38. Singnurkar A, Poon R, Detsky J. 18F-FET-PET imaging in high-grade gliomas and brain metastases: A systematic review and meta-analysis. J Neurooncol. 2023; 161: 1-12.
39. Lapa C, Linsenmann T, Monoranu CM, Samnick S, Buck AK, Bluemel C, et al. Comparison of the amino acid tracers 18F-FET and 18F-DOPA in high-grade glioma patients. J Nucl Med. 2014; 55: 1611-6.
40. Chondrogiannis S, Marzola MC, Al-Nahhas A, Venkatanarayana TD, Mazza A, Opocher G, et al. Normal biodistribution pattern and physiologic variants of 18F-DOPA PET imaging. Nucl Med Comm. 2013; 34: 1141.
41. Rufini V, Treglia G, Montravers F, Giordano A. Diagnostic accuracy of [18F] DOPA PET and PET/CT in patients with neuroendocrine tumors: a meta-analysis. Clin Transl Imaging. 2013; 1: 111-22.
42. Piccardo A, Fiz F, Bottoni G, Ugolini M, Noordzij W, Trimboli P. Head-to-head comparison between 18F-DOPA PET/CT and 68Ga-DOTA peptides PET/CT in detecting intestinal neuroendocrine tumours: A systematic review and meta-analysis. Clin Endocrinol. 2021; 95: 595-605.
43. Treglia G, Cocciolillo F, Di Nardo F, Poscia A, de Waure C, Giordano A, et al. Detection Rate of Recurrent Medullary Thyroid Carcinoma Using Fluorine-18 Dihydroxyphenylalanine Positron Emission Tomography: A Meta-analysis. Acad Radiol. 2012; 19: 1290-9.
44. Xiao J, Jin Y, Nie J, Chen F, Ma X. Diagnostic and grading accuracy of 18F-FDOPA PET and PET/CT in patients with gliomas: A systematic review and meta-analysis. BMC Cancer. 2019; 19: 767.
45. Okudaira H, Nakanishi T, Oka S, Kobayashi M, Tamagami H, Schuster DM, et al. Kinetic analyses of trans-1-amino-3-[18F]fluorocyclobutanecarboxylic acid transport in *Xenopus laevis* oocytes expressing human ASCT2 and SNAT2. Nucl Med Biol. 2013; 40: 670-5.
46. Nye JA, Schuster DM, Yu W, Camp VM, Goodman MM, Votaw JR. Biodistribution and Radiation Dosimetry of the Synthetic Nonmetabolized Amino Acid Analogue Anti-18F-FACBC in Humans. J Nucl Med. 2007; 48: 1017-20.
47. Seierstad T, Hole KH, Tulipan AJ, Strømme H, Lilleby W, Revheim M-E, et al. 18F-Fluciclovine PET for Assessment of Prostate Cancer with Histopathology as Reference Standard: A Systematic Review. PET Clin. 2021; 16: 167-76.
48. Alberts IL, Seide SE, Mingels C, Bohn KP, Shi K, Zacho HD, et al. Comparing the diagnostic performance of radiotracers in recurrent prostate cancer: A systematic review and network meta-analysis. Eur J Nucl Med. 2021; 48: 2978-89.
49. Castello A, Albano D, Muoio B, Castellani M, Panareo S, Rizzo A, et al. Diagnostic Accuracy of PET with 18F-Fluciclovine ([18F]FACBC) in Detecting High-Grade Gliomas: A Systematic Review and Meta-Analysis. Diagnostics. 2023; 13: 3610.
50. Inoue T, Koyama K, Oriuchi N, Alyafei S, Yuan Z, Suzuki H, et al. Detection of malignant tumors: whole-body PET with fluorine-18 alpha-methyl tyrosine versus FDG: Preliminary study. Radiology. 2001; 220: 54-62.
51. Achmad A, Bhattarai A, Yudistiro R, Heryanto YD, Higuchi T, Tsushima Y. The diagnostic performance of 18F-FAMT PET and 18F-FDG PET for malignancy detection: A meta-analysis. BMC Med Imaging. 2017; 17: 66.
52. Yanagida O, Kanai Y, Chairoungdua A, Kim DK, Segawa H, Nii T, et al. Human L-type amino acid transporter 1 (LAT1): characterization of function and expression in tumor cell lines. Biochim Biophys Acta. 2001; 1514: 291-302.

53. Stegink LD, Filer LJ, Jr., Brummel MC, Baker GL, Krause WL, Bell EF, et al. Plasma amino acid concentrations and amino acid ratios in normal adults and adults heterozygous for phenylketonuria ingesting a hamburger and milk shake meal. Am J Clin Nutr. 1991; 53: 670-5.
54. Uchino H, Kanai Y, Kim DK, Wempe MF, Chairoungdua A, Morimoto E, et al. Transport of amino acid-related compounds mediated by L-type amino acid transporter 1 (LAT1): Insights into the mechanisms of substrate recognition. Mol Pharmacol. 2002; 61: 729-37.
55. Ishiwata K, Ido T, Mejia AA, Ichihashi M, Mishima Y. Synthesis and radiation dosimetry of 4-borono-2-[^{18}F]fluoro-d,l-phenylalanine: A target compound for PET and boron neutron capture therapy. Int J Rad Appl Instr A. 1991; 42: 325-8.
56. Zhou T, Igawa K, Kasai T, Sadahira T, Wang W, Watanabe T, et al. The current status and novel advances of boron neutron capture therapy clinical trials. Am J Cancer Res. 2024; 14: 429-47.
57. Ishiwata K. 4-Borono-2-^{18}F-fluoro-L-phenylalanine PET for boron neutron capture therapy-oriented diagnosis: Overview of a quarter century of research. Ann Nucl Med. 2019; 33: 223-36.
58. Chang T-Y, Chang W-Y, Chen Y-W, Ho M-C, Chang C-W, Lau S-O, et al. Comparison of the synthesis and biological properties of no-carrier-added and carrier-added 4-borono-2-[^{18}F]fluorophenylalanine ([^{18}F]FBPA). Nucl Med Biol. 2023; 116-117: 108313.
59. Ishiwata K, Shiono M, Kubota K, Yoshino K, Hatazawa J, Ido T, et al. A unique in vivo assessment of 4-[^{10}B]borono-L-phenylalanine in tumour tissues for boron neutron capture therapy of malignant melanomas using positron emission tomography and 4-borono-2-[^{18}F]fluoro-L-phenylalanine. Melanoma Res. 1992; 2: 171-80.
60. Yang Q, Zhu W, Ren C, Ji H, Wang D, Liu Y, et al. Biodistribution and radiation dosimetry of D-isomer of 4-borono-2-[^{18}F]fluoro-phenylalanine: A comparative PET/CT study with L-isomer in healthy human volunteers. Nucl Med Biol. 2021; 94-95: 32-7.
61. Hirai N, Watabe T, Nagamori S, Wiriyasermkul P, Tanaka Y, Romanov V, et al. Evaluation of D-isomer of ^{18}F-FBPA for oncology PET focusing on the differentiation of glioma and inflammation. Asia Ocean J Nucl Med Biol. 2020; 8: 102-8.
62. Wongthai P, Hagiwara K, Miyoshi Y, Wiriyasermkul P, Wei L, Ohgaki R, et al. Boronophenylalanine, a boron delivery agent for boron neutron capture therapy, is transported by ATB$^{0,+}$, LAT1 and LAT2. Cancer Sci. 2015; 106: 279-86.
63. Harada S, Kajihara R, Muramoto R, Jutabha P, Anzai N, Nemoto T. Catalytic asymmetric synthesis of alpha-methyl-p-boronophenylalanine. Bioorg Med Chem Lett. 2018; 28: 1915-8.
64. Watabe T, Ikeda H, Nagamori S, Wiriyasermkul P, Tanaka Y, Naka S, et al. ^{18}F-FBPA as a tumor-specific probe of L-type amino acid transporter 1 (LAT1): a comparison study with ^{18}F-FDG and ^{11}C-Methionine PET. Eur J Nucl Med Mol Imaging. 2017; 44: 321-31.
65. Shimosegawa E, Isohashi K, Naka S, Horitsugi G, Hatazawa J. Assessment of ^{10}B concentration in boron neutron capture therapy: potential of image-guided therapy using ^{18}FBPA PET. Ann Nucl Med. 2016; 30: 749-55.
66. Watabe T, Ose N, Naka S, Fukui E, Kimura T, Kanou T, et al. Evaluation of LAT1 Expression in Patients With Lung Cancer and Mediastinal Tumors: ^{18}F-FBPA PET Study With Immunohistological Comparison. Clin Nucl Med. 2023; 48: 853-60.
67. Watabe T, Shimamoto H, Naka S, Kamiya T, Murakami S. ^{18}F-FBPA PET in Sarcoidosis: Comparison to Inflammation-Related Uptake on FDG PET. Clin Nucl Med. 2020; 45: 863-4.
68. Tani H, Kurihara H, Hiroi K, Honda N, Yoshimoto M, Kono Y, et al. Correlation of ^{18}F-BPA and ^{18}F-FDG uptake in head and neck cancers. Radiother Oncol. 2014; 113: 193-7.
69. Igaki H, Nakamura S, Kurihara H, Abe Y, Nishioka S, Fujii R, et al. Comparison of ^{18}FBPA uptake with ^{18}FDG uptake in cancer patients. Appl Radiat Isot. 2020; 157: 109019.
70. Nakaichi T, Nakamura S, Ito K, Takahashi K, Takemori M, Kashihara T, et al. Analyzing spatial distribution between ^{18}F-fluorodeoxyglucose and ^{18}F-boronophenylalanine positron emission tomography to investigate selection indicators for boron neutron capture therapy. EJNMMI Phys. 2022; 9: 89.
71. Isohashi K, Kanai Y, Aihara T, Hu N, Fukushima K, Baba I, et al. Exploration of the threshold SUV for diagnosis of malignancy using ^{18}F-FBPA PET/CT. Eur J Hybrid Imaging. 2022; 6: 35.
72. Kashihara T, Mori T, Nakaichi T, Nakamura S, Ito K, Kurihara H, et al. Correlation between L-amino acid transporter 1 expression and 4-borono-2-^{18}F-fluoro-phenylalanine accumulation in humans. Cancer Med. 2023; 12: 20564-72.
73. Li J, Shi Y, Zhang Z, Liu H, Lang L, Liu T, et al. A metabolically stable boron-derived tyrosine serves as a theranostic agent for positron emission tomography guided boron neutron capture therapy. Bioconjugate Chem. 2019; 30: 2870-8.
74. Li Z, Kong Z, Chen J, Li J, Li N, Yang Z, et al. ^{18}F-Boramino acid PET/CT in healthy volunteers and glioma patients. Eur J Nucl Med Mol Imaging. 2021; 48: 3113-21.
75. Kong Z, Li Z, Chen J, Liu S, Liu D, Li J, et al. Metabolic characteristics of [^{18}F]fluoroboronotyrosine (FBY) PET in malignant brain tumors. Nucl Med Biol. 2022; 106-107: 80-7.
76. Kong Z, Li Z, Chen J, Ma W, Wang Y, Yang Z, et al. Larger ^{18}F-fluoroboronotyrosine (FBY) active volume beyond MRI contrast enhancement in diffuse gliomas than in circumscribed brain tumors. EJNMMI Res. 2022; 12: 22.
77. Li Z, Chen J, Kong Z, Shi Y, Xu M, Mu B-S, et al. A bis-boron boramino acid PET tracer for brain tumor diagnosis. Eur J Nucl Med Mol Imaging. 2024; 51: 1703-12.
78. Kong Z, Li Z, Chen J, Shi Y, Li N, Ma W, et al. A histogram of [^{18}F]BBPA PET imaging differentiates non-neoplastic lesions from malignant brain tumors. EJNMMI Research. 2024; 14: 12.
79. Langen K-J, Ziemons K, Kiwit JC, Herzog H. 3-(^{123}I) Iodo-alpha-methyltyrosine and (methyl-^{11}C)-L-methionine uptake in cerebral gliomas: A comparative study using SPECT and PET. J Nucl Med. 1997; 38: 517.
80. Shikano N, Kanai Y, Kawai K, Inatomi J, Kim DK, Ishikawa N, et al. Isoform selectivity of 3-^{125}I-iodo-α-methyl-L-tyrosine membrane transport in human L-type amino acid transporters. J Nucl Med. 2003; 44: 244-6.
81. Shikano N, Kawai K, Nakajima S, Nishii R, Flores II LG, Kubodera A, et al. Renal accumulation and excretion of radioiodinated 3-iodo-α-methyl-L-tyrosine. Ann Nucl Med. 2004; 18: 263-70.
82. Tomiyoshi K, Amed K, Muhammad S, Higuchi T, Inoue T, Endo K, et al. Synthesis of isomers of ^{18}F-labelled amino acid radiopharmaceutical: position 2- and 3-L-^{18}F-α-methyltyrosine using a separation and purification system. Nucl Med Commun. 1997; 18: 169-75.
83. Amano S, Inoue T, Tomiyoshi K, Ando T, Endo K. In vivo comparison of PET and SPECT radiopharmaceuticals in detecting breast cancer. J Nucl Med. 1998; 39: 1424-7.
84. Meleán JC, Humpert S, Ermert J, Coenen HH. Stereoselective radiosynthesis of L- and D-3-[^{18}F]fluoro-α-methyltyrosine. J Fluor Chem. 2015; 178: 202-7.
85. Aoki M, Watabe T, Nagamori S, Naka S, Ikeda H, Kongpracha P, et al. Distribution of LAT1-targeting PET tracer was independent of the tumor blood flow in rat xenograft models of C6 glioma and MIA PaCa-2. Ann Nucl Med. 2019; 33: 394-403.
86. Yamaguchi A, Hanaoka H, Higuchi T, Tsushima Y. Selective synthesis of L-2-[^{18}F]fluoro-alpha-methylphenylalanine via copper-mediated ^{18}F-fluorination of (mesityl)(aryl)iodonium salt. J Labelled Comp Radiopharm. 2020; 63: 368-75.
87. Ohshima Y, Hanaoka H, Tominaga H, Kanai Y, Kaira K, Yamaguchi A, et al. Biological evaluation of 3-[^{18}F]fluoro-α-methyl-D-tyrosine (D-[^{18}F]FAMT) as a novel amino acid tracer for positron emission tomography. Ann Nucl Med. 2013; 27: 314-24.
88. Sakai T, Watabe T, Hirai N, Tani N, Ikeda H, Naka S, et al. Evaluation of LAT1 tracer ^{18}F-FAMT in the inflammatory lesions -comparison study with ^{18}F-FDG PET. J Nucl Med. 2018; 59: 1108.
89. Yamaguchi A, Hanaoka H, Fujisawa Y, Zhao S, Suzue K, Morita A, et al. Differentiation of malignant tumours from granulomas by using dynamic [^{18}F]-fluoro-L-α-methyltyrosine positron emission tomography. EJNMMI Res. 2015; 5: 1-8.
90. Kim M, Achmad A, Higuchi T, Arisaka Y, Yokoo H, Yokoo S, et al. Effects of Intratumoral Inflammatory Process on ^{18}F-FDG Uptake: Pathologic and Comparative Study with ^{18}F-Fluoro-α-Methyltyrosine PET/CT in Oral Squamous Cell Carcinoma. J Nucl Med. 2015; 56: 16-21.
91. Yudistiro R, Arisaka Y, Tokue A, Nakajima T. Differentiation of sarcoidosis-lymphoma syndrome lesions: a case report on the use of two different positron emission tomography tracers. BMC Med Imaging. 2016; 16: 1.
92. Horiguchi K, Tosaka M, Higuchi T, Arisaka Y, Sugawara K, Hirato J, et al. Clinical value of fluorine-18α-methyltyrosine PET in patients with gliomas: comparison with fluorine-18 fluorodeoxyglucose PET. EJNMMI Research. 2017; 7: 50.
93. Kumasaka S, Nakajima T, Arisaka Y, Tokue A, Achmad A, Fukushima Y, et al. Prognostic value of metabolic tumor volume of pretreatment ^{18}F-FAMT PET/CT in non-small cell lung cancer. BMC Med Imaging. 2018; 18: 46.
94. Sohda M, Honjyo H, Hara K, Ozawa D, Suzuki S, Tanaka N, et al. L-[3-^{18}F]-α-Methyltyrosine Accumulation as a Definitive Chemoradiotherapy Response Predictor in Patients with Esophageal Cancer. Anticancer Res. 2014; 34: 909-13.

95. Kim M, Higuchi T, Nakajima T, Andriana P, Hirasawa H, Tokue A, et al. ^{18}F-FDG and ^{18}F-FAMT PET-derived metabolic parameters predict outcome of oral squamous cell carcinoma. Oral Radiol. 2019; 35: 308-14.
96. Wei L, Tominaga H, Ohgaki R, Wiriyasermkul P, Hagiwara K, Okuda S, et al. Transport of 3-fluoro-l-α-methyl-tyrosine (FAMT) by organic ion transporters explains renal background in [^{18}F]FAMT positron emission tomography. J Pharmacol Sci. 2016; 120: 101-9.
97. Kanai A, Hanaoka H, Yamaguchi A, Mahendra I, Palangka C, Ohshima Y, et al. Enhancing the accumulation level of 3-[^{18}F]fluoro-L-α-methyltyrosine in tumors by preloading probenecid. Nucl Med Biol. 2022; 104-105: 47-52.
98. Faried A, Bolly HMB, Hermanto Y, Achmad A, Halim D, Tjahjono FP, et al. Prognostic significance of L-type amino acid transporter-1 (LAT-1) expression in human astrocytic gliomas. Interdiscip Neurosurg. 2021; 23: 100939.
99. Albert NL, Winkelmann I, Suchorska B, Wenter V, Schmid-Tannwald C, Mille E, et al. Early static ^{18}F-FET-PET scans have a higher accuracy for glioma grading than the standard 20–40 min scans. Eur J Nucl Med Mol Imaging. 2016; 43: 1105-14.
100. Ohshima Y, Hanaoka H, Watanabe S, Sugo Y, Watanabe S, Tominaga H, et al. Preparation and biological evaluation of 3-[^{76}Br]bromo-alpha-methyl-L-tyrosine, a novel tyrosine analog for positron emission tomography imaging of tumors. Nucl Med Biol. 2011; 38: 857-65.
101. Hanaoka H, Ohshima Y, Suzuki Y, Yamaguchi A, Watanabe S, Uehara T, et al. Development of a Widely Usable Amino Acid Tracer: ^{76}Br-α-Methyl-Phenylalanine for Tumor PET Imaging. J Nucl Med. 2015; 56: 791-7.
102. Mahendra I, Hanaoka H, Yamaguchi A, Amartuvshin T, Tsushima Y. Diagnosis of bladder cancer using ^{18}F-labeled alpha-methyl-phenylalanine tracers in a mouse model. Ann Nucl Med. 2020; 34: 329-36.
103. Ohshima Y, Suzuki H, Hanaoka H, Sasaki I, Watanabe S, Haba H, et al. Preclinical evaluation of new α-radionuclide therapy targeting LAT1: 2-[^{211}At]astato-α-methyl-L-phenylalanine in tumor-bearing model. Nucl Med Biol. 2020; 90-91: 15-22.
104. Hanaoka H, Ohshima Y, Suzuki H, Sasaki I, Watabe T, Ooe K, et al. Enhancing the Therapeutic Effect of 2-^{211}At-astato-α-methyl-L-phenylalanine with Probenecid Loading. Cancers. 2021; 13: 5514.
105. Hanaoka H, Ohshima Y, Yamaguchi A, Suzuki H, Ishioka NS, Higuchi T, et al. Novel ^{18}F-Labeled α-Methyl-Phenylalanine Derivative with High Tumor Accumulation and Ideal Pharmacokinetics for Tumor-Specific Imaging. Mol Pharm. 2019; 16: 3609-16.
106. Nozaki S, Nakatani Y, Mawatari A, Shibata N, Hume WE, Hayashinaka E, et al. ^{18}F-FIMP: a LAT1-specific PET probe for discrimination between tumor tissue and inflammation. Sci Rep. 2019; 9: 15718.
107. Nozaki S, Nakatani Y, Mawatari A, Hume WE, Doi H, Watanabe Y. In vitro evaluation of *(S)*-2-amino-3-[3-(2-^{18}F-fluoroethoxy)-4-iodophenyl]-2-methylpropanoic acid (^{18}F-FIMP) as a positron emission tomography probe for imaging amino acid transporters. EJNMMI Res. 2023; 13: 36.
108. Lu Y, Jiang Z, Wang K, Yu S, Hao C, Ma Z, et al. Blockade of the amino acid transporter SLC6A14 suppresses tumor growth in colorectal Cancer. BMC Cancer. 2022; 22: 833.
109. Nozaki S, Nakatani Y, Mawatari A, Hume WE, Wada Y, Ishii A, et al. First-in-human assessment of the novel LAT1 targeting PET probe ^{18}F-FIMP. Biochem Biophys Res Commun. 2022; 596: 83-7.
110. Treglia G, Muoio B, Trevisi G, Mattoli MV, Albano D, Bertagna F, et al. Diagnostic Performance and Prognostic Value of PET/CT with Different Tracers for Brain Tumors: A Systematic Review of Published Meta-Analyses. Int J Mol Sci. 2019; 20: 4669.
111. Guarch ME, Font-Llitjós M, Murillo-Cuesta S, Errasti-Murugarren E, Celaya AM, Girotto G, et al. Mutations in L-type amino acid transporter-2 support SLC7A8 as a novel gene involved in age-related hearing loss. Elife. 2018; 7: e31511.
112. Ninatti G, Pini C, Gelardi F, Sollini M, Chiti A. The Role of PET Imaging in the Differential Diagnosis between Radiation Necrosis and Recurrent Disease in Irradiated Adult-Type Diffuse Gliomas: A Systematic Review. Cancers. 2023; 15: 364.
113. Zwart PLd, Dijken BRJv, Holtman GA, Stormezand GN, Dierckx RA, Laar PJv, et al. Diagnostic accuracy of positron emission tomography tracers for the differentiation of tumor progression from treatment-related changes in high-grade glioma: a systematic review and meta-analysis. J Nucl Med. 2020; 61: 498-504.
114. Schlürmann T, Waschulzik B, Combs S, Gempt J, Wiestler B, Weber W, et al. Utility of Amino Acid PET in the Differential Diagnosis of Recurrent Brain Metastases and Treatment-Related Changes: A Meta-analysis. J Nucl Med. 2023; 64: 816.
115. Nozaki S, Nakatani Y, Mawatari A, Shibata N, Hume WE, Hayashinaka E, et al. Comparison of [^{18}F]FIMP, [^{11}C]MET, and [^{18}F]FDG PET for early-phase assessment of radiotherapy response. Sci Rep. 2023; 13: 1961.
116. Wang L, Qu W, Lieberman BP, Plössl K, Kung HF. Synthesis, uptake mechanism characterization and biological evaluation of ^{18}F labeled fluoroalkyl phenylalanine analogs as potential PET imaging agents. Nucl Med Biol. 2011; 38: 53-62.
117. Verhoeven J, Hulpia F, Kersemans K, Bolcaen J, De Lombaerde S, Goeman J, et al. New fluoroethyl phenylalanine analogues as potential LAT1-targeting PET tracers for glioblastoma. Sci Rep. 2019; 9: 2878.
118. Verhoeven J, Baguet T, Piron S, Pauwelyn G, Bouckaert C, Descamps B, et al. 2-[^{18}F]FELP, a novel LAT1-specific PET tracer, for the discrimination between glioblastoma, radiation necrosis and inflammation. Nucl Med Biol. 2020; 82-83: 9-16.
119. Wempe MF, Jutabha P, Kumar V, Fisher JA, Waers K, Holt MD, et al. Developing selective L-Amino Acid Transport 1 (LAT1) inhibitors: A structure-activity relationship overview. Med Res Arch. 2019; 7.
120. Oda K, Hosoda N, Endo H, Saito K, Tsujihara K, Yamamura M, et al. L-type amino acid transporter 1 inhibitors inhibit tumor cell growth. Cancer Sci. 2010; 101: 173-9.
121. [Internet] J-Pharma Development Pipeline. 2023 Accessed November 2, 2024. https://www.j-pharma.com/en/developmentpipeline/
122. Naka S, Watabe T, Kanai Y, Nagamori S, Kurimoto K, Kato H, et al. Automated synthesis of [^{18}F]NKO-035 as a novel L-type amino acid transporter 1 (LAT1) tracer for human use. J Nucl Med. 2020; 61 (Suppl 1): S1130.
123. Kanai Y, Watabe T, Nagamori S, Naka S, Sakai T, Kato H, et al. Radiosynthesis and basic evaluation of [^{18}F]NKO-028 as a L-type amino acid transporter 1 (LAT1) PET tracer for cancer diagnosis. J Nucl Med. 2016; 57 (Suppl 2): S1185.
124. Katayama D, Watabe T, Nagamori S, Kanai Y, Naka S, Liu Y, et al. Preclinical evaluation of new PET tracer targeting L-type Amino Acid Transporter 1(LAT1): F-18 NKO-035 PET in inflammation model of rats. J Nucl Med. 2018; 59 (Suppl 1): S1121.
125. Watabe T, Naka S, Soeda F, Kamiya T, Sasaki H, Katayama D, et al. First in human dosimetry of ^{18}F-NKO-035: a new PET probe targeting L-type amino acid transporter 1 (LAT1). J Nucl Med. 2020; 61 (Suppl 1): S627.
126. Paiva FG, Santana PdC, Mourão AP. Evaluation of patient effective dose in a PET/CT test. Appl Radiat Isot. 2019; 145: 137-41.
127. [Internet] Safety of novel cancer-specific PET probe confirmed in clinical research. 2019. Accessed November 2, 2024. https://resou.osaka-u.ac.jp/en/research/2019/20191224_2
128. [Internet] Usefulness evaluation of PET probe F18-NKO-035. 2020. Accessed November 2, 2024. https://rctportal.niph.go.jp/en/detail?trial_id=jRCTs051200075
129. Singh N, Scalise M, Galluccio M, Wieder M, Seidel T, Langer T, et al. Discovery of potent inhibitors for the large neutral amino acid transporter 1 (LAT1) by structure-based methods. Int J Mol Sci. 2019; 20: 27.

Author Biography

Dr. Arifudin Achmad is an assistant professor of nuclear medicine and molecular theranostics at the Faculty of Medicine, Universitas Padjadjaran, Indonesia. He has co-authored over 20 peer-reviewed publications in nuclear medicine journals, including the *Journal of Nuclear Medicine* and the *European Journal of Nuclear Medicine and Molecular Imaging*. He holds two Indonesian patents and received grants in molecular modeling of LAT1-targeting compounds.

Dr. Hirofumi Hanaoka is a professor of radiotheranostics at Kansai Medical University, Japan. He was Dr. Arifudin's supervisor while pursuing a doctoral degree at Gunma University. Dr. Hanaoka obtained multiple grants in radioimmuno-imaging/therapy and photoimmunotherapy research. He has published articles in top chemistry journals such as *Nanomedicine*, *Molecular Cancer Therapeutics*, *Molecular Oncology*, and *Bioconjugate Chemistry*.

Dr. Holis Abdul Holik is an associate professor of medicinal chemistry at the Faculty of Pharmacy, Universitas Padjadjaran. He earned his PhD at the Department of Molecular Imaging and Radiotherapy, Chiba University. He holds three Indonesian patents and received grants in molecular modeling of LAT1-targeting compounds.

Prof. Keigo Endo is a professor emeritus of nuclear medicine at Gunma University, Japan. He is the former president of the Japan Radiological Society and the Japanese Society of Nuclear Medicine. Professor Endo was Dr. Arifudin's mentor while pursuing a doctoral degree at Gunma University. He had multiple publications in top nuclear medicine journals. Currently, Prof. Endo is the president of Kyoto College of Medical Science.

Prof. Yoshito Tsushima is a professor of diagnostic radiology at Gunma University, Japan. He has publications in top radiology journals such as the *British Journal of Radiology* and the *European Journal of Radiology*. He mentored Dr. Arifudin when he enrolled in the post-doctoral program and performed cancer-targeting nanocapsule research at Gunma University.

Prof. Achmad Hussein S. Kartamihardja is a professor of nuclear medicine and molecular theranostics at the Faculty of Medicine, Universitas Padjadjaran/Hasan Sadikin General Hospital, Indonesia. He is one of the founders and former president of the Indonesian Society of Nuclear Medicine and Molecular Theranostics. He is one of the regional representatives (Vice Presidents) of the Asia Oceania Federation of Nuclear Medicine and Biology. He holds multiple Indonesian patents and received multi-year research grants for developing LAT1-targeting radiopharmaceuticals.